A Semi-Analytical Analysis of Gas Slippage Effect in Pressure Transient Behavior of Non-Condensate Gas Reservoirs with the Different Boundary Condition

Sheikhi, Sobhan*[+]

Skolkovo Institute of Science and Technology, Moscow, RUSSIAN FEDERATION

ABSTRACT: *The conventional models utilized to study flow behavior in a Non-Condensate gas reservoir did not consider the effects of gas slippage and different outer boundary conditions. For gas wells with a constant production flow rate in a bounded oil or gas reservoir, commonly, the outer boundary conditions are infinite boundary conditions or zero flux. In this study, the dimensionless pseudo pressure and dimensionless derivative of pseudo pressure in the presence of 4 different outer boundary conditions (infinite reservoir, constant pressure, exponential, and power-law) besides effects of gas slippage, wellbore storage, and skin factor are analyzed. To do this, the dimensionless pseudo pressure partial differential equation of radial flow was derived from the combination of continuity equation with Darcy's law, the equation of state, compressibility equation, and dimensionless parameters. Then the derived partial differential equation is solved analytically in the Laplace domain. The obtained results of this work have important significance to understand the effects of different conditions on the transient pressure behavior of Non-Condensate gas reservoirs.*

KEYWORDS: *Pressure transient analysis; Non-condensate gas reservoirs; Boundary conditions; Gas slippage*

INTRODUCTION

Simulation of fluid flow in porous media is an important aspect of many different fields of studies [1-3]. Engineers who deal with porous media must have adequate data about in-situ porous media (reservoir) conditions. Relative permeability (which is controlled by wettability), permeability, and porosity are some fundamental characteristic of porous media which in large scale for hydrocarbon reservoirs are determined by petroleum engineers with the aid of the well-test technique [4-8]. The significance of the transient flow of a fluid is well-known and many techniques are available for estimating well pressure response in different well configurations, reservoir fluid, and reservoir geometry [9, 10]. Investigation of pressure response of reservoir with different fluids; such as dry gas [11], gas condensate reservoirs [12], and oil reservoir [11], as well as unusual well configuration such as horizontal well [13], and hydraulic fractured wells [14], are some example of tremendous studies in the well-test analysis. However, a fully penetrating well usually with a constant flow rate situated at the center of a cylindrical porous media is a typical model utilized to investigate the transition flow behavior of gas and oil wells [6, 15, 16].

* *To whom correspondence should be addressed.*
+ *E-mail: Sobhan.sheikhi@skoltech.ru*
1021-9986/2021/1/333-341 9/$/5.09

However, well-test interpretations are subjected to error because of the different effects of well and external boundary conditions [17, 18]. For homogeneous underground oil reservoirs, the wellbore pressure transition behavior affected by the external boundary conditions for instances faults, constant pressure, and no flow has been considered and analyzed in several studies [19, 20]. *Pascal* and *Pascal* [1] modeled the flow behavior in porous materials and they considered a moving external boundary to simulate the unsteady-state flow regime of non-Newtonian (power-law) fluids. *Acosta* and *Ambastha* [19] general method analyzed the pressure transient behavior for a composite underground oil reservoir with a fractal region between the homogeneous circular regions. Corbett et al. [21] through considering vertical influx to reservoir presented a new pressure transition response model. *Doublet* and *Blasingame* [22] numerically analyzed the well test of reservoir influenced by a variable flow condition at the outer boundary.

Modeling and analyzing various gaseous flow regimes through low permeability reservoirs because of the weakness of Darcy's law in a realistic description of the flow regimes other than the viscous flow has been subjected to considerable studies [23, 24]. In these reservoirs, the diameter of the pore throat usually ranges from few nanometers to 1μm [25, 26]. Recently, some studies even disclosed sub-nanometer pores inside the mentioned reservoirs [27, 28]. Extremely small pores resulted in very different transport mechanisms of fluid flows in unconventional reservoirs in comparison with conventional reservoirs [29]. *Javadpour et al.* [30] showed that gas flow in shale deviates from Fick's and Darcy's equation. Therefore, many researchers tried to describe the transfer of gas through low permeability porous media under various conditions. However, there is a lack of study in previous works in considering the slippage effect beside different boundary conditions. Hence, this study tries to complete previous studies by incorporating the developed models for flow in tight gas in pressure transient behavior studies. Gas flow studies coupled with slippage effects at the solid wall, initially addressed by *Maxwell* [31]. Klinkenberg formulation of gas slippage and permeability modification of porous media is one of the primary studies in gas slippage researches [31]. Generally, the gas slippage effect should be considered as the mean free path of a gas molecule is within four orders of magnitude of the pore-throat radius (0.1<Knudsen number<1) [32]. Hence, the gas slippage effect increases in low-permeability reservoirs.

In this study, a time-dependent variable condition (power-law and exponential) and constant condition (infinite-acting reservoir and constant pressure) at the external boundary is proposed. A semi-analytical solution is achieved for analyzing and interoperating dimensionless pseudo pressure and its derivative behavior in Non-Condensate gas reservoirs. The pressure responses of these work for different boundary conditions are compared with each other. The physical model of the reservoir is a single well centered in a circular underground Non-Condensate gas reservoir with four various external boundary conditions along with slippage, wellbore storage, and skin factor effect.

THEORETICAL SECTION

The continuity equation in a radial coordinate can be described as below [4],

$$\rho q|_{r+dr} - \rho q|_{r} = \frac{\partial(\rho V \phi)}{\partial t} \tag{1}$$

Where ρ, q, Φ, V, and t are density, flow rate, volume, porosity, and time, respectively. The volume of the element in a radial coordinate is defined as,

$$V = 2\pi rhdr \tag{2}$$

Where r, h, dr are radial distance, thickness, and element width. The radial flow rate is defined as,

$$q_r = v_r A_r \tag{3}$$

The cross-section area $A_r = 2\pi rh$. By substituting cross-section and flow rate in equation (1), the below equation is achieved,

$$\frac{\rho r v|_{r+dr} - \rho r v|_{r}}{rdr} = \frac{\partial(\rho\phi)}{\partial t} \tag{4}$$

The velocity in r direction based on Darcy's law is [33],

$$v_r = \frac{k_{r,a}}{\mu}\frac{\partial p}{\partial r} \tag{5}$$

Where k_a and μ are apparent permeability and viscosity, respectively. The relation between gas slippage and absolute permeability is [30],

$$k_a = k_\infty B \tag{6}$$

Where k_∞ and B are absolute permeability and a coefficient of dependent to Knudsen number, respectively. The B can be related to Knudsen number (K_n) as,

$$B = 1 + f(K_n) \tag{7}$$

Where f is a function dependent on the Knudsen number. The density of the gas is based on the equation of state and is calculated as [15],

$$\rho_g = \frac{M}{RT}\frac{p}{z_g} \tag{8}$$

Where M, R, T, and z_g are gas molecular weight, the universal constant of gas, temperature, and deviation factor of gas, respectively. By substituting equations of (5), (6) and (8) in equation (4),

$$\frac{\partial\left(\frac{M}{RT}\frac{p}{z_g} r \frac{k_{r,\infty} B}{\mu}\frac{\partial p}{\partial r}\right)}{r\partial r} = \frac{\partial\left(\frac{M}{RT}\frac{p}{z_g}\phi\right)}{\partial t} \tag{9}$$

Simplifying equation (9) results in,

$$k_{r,\infty} B \frac{\partial(r\frac{p}{z_g\mu}\frac{\partial p}{\partial r})}{r\partial r} = \frac{\partial(\frac{p}{z_g}\phi)}{\partial t} \tag{10}$$

Gas pseudo pressure is defined as [17],

$$m = 2\int_{p_0}^{p} \frac{p}{\mu z_g} dp \tag{11}$$

Or

$$\frac{\mu z_g}{2p}\frac{\partial m}{\partial u} = \frac{\partial p}{\partial u} \tag{12}$$

The isothermal coefficient of gas compressibility and reservoir compressibility are, respectively,

$$c_g = \frac{1}{p} - \frac{1}{z_g}(\frac{\partial z_g}{\partial p})_T \tag{13}$$

$$C_f = \frac{1}{\phi}\frac{\partial \phi}{\partial p} \tag{14}$$

With the aims of chain role [34],

$$\frac{\partial}{\partial t}(\frac{p}{z_g}) = \frac{\partial}{\partial p}(\frac{p}{z_g}) * \frac{\partial p}{\partial t} = \tag{15}$$

$$\frac{p}{z}(\frac{1}{p} - \frac{1}{z_g}\frac{\partial z_g}{\partial p}) = \frac{p}{z_g} c_g \frac{\partial p}{\partial t}$$

Simplifying equation (15),

$$k_{r,\infty} B \frac{\partial(r\frac{\partial \psi}{\partial r})}{r\partial r} = \mu c_t \phi \frac{\partial \psi}{\partial t} \tag{16}$$

Separating different terms of equation (16) results in,

$$k_{r,\infty} B \frac{\partial^2 \psi}{\partial r^2} + \frac{k_{r,\infty} B}{r}\frac{\partial \psi}{\partial r} = \mu c_t \phi \frac{\partial \psi}{\partial t} \tag{17}$$

Dimensionless parameters are defined as follows,

$$r_D = \frac{r}{L_{re}} \quad , \; L_{re} = x_f \quad , t_D = \frac{kt}{\phi \mu c_t r_w^{\,2}} \tag{18}$$

As we consider the reservoir is axisymmetric, then it can be solved just in r direction, by this assumption and substituting dimensionless parameters,

$$\frac{\partial^2 m_D}{\partial r_D^{\,2}} + \frac{1}{r_D}\frac{\partial m_D}{\partial r_D} = \frac{1}{B}\frac{\partial m_D}{\partial t_D} \tag{19}$$

Taking the Laplace transform of equation (19)

$$\frac{\partial^2 \overline{m}_D}{\partial r_D^{\,2}} + \frac{1}{r_D}\frac{\partial \overline{m}_D}{\partial r_D} - \frac{s}{B}\overline{m}_D = 0 \tag{20}$$

Through defining a new variable of $w = \sqrt{s/B}\, r_{eD}$, a new form of equation (20) became as follow,

$$\frac{s}{B}\frac{\partial^2 \overline{m}_D}{\partial w^2} + \frac{s}{Bw}\frac{\partial \overline{m}_D}{\partial w} - \frac{s}{B}\overline{m}_D = 0 \tag{21}$$

More simplifying of equation (21) results in,

$$w^2 \frac{\partial^2 \overline{m}_D}{\partial w^2} + w\frac{\partial \overline{m}_D}{\partial w} - w^2 \overline{m}_D = 0 \tag{22}$$

Generally, a solution in the form of modified Bessel function for equation (22) is [35],

$$\overline{m}_D = c_1 I_0(w) + c_2 k_0(w) \tag{23}$$

Where I_0, k_0, c_1, and c_2 are zero-order modified Bessel function of the first kind, zero-order modified Bessel function of the second kind, first constant and second constant, respectively. To achieve c_1 and c_2 the boundary conditions should be applied. For the outer boundary, four different boundary condition is considered.

1) Infinite reservoir ($\frac{\partial \overline{m}_D(r_D \to \infty, t_D)}{\partial r_D} = 0$),

2) constant pressure reservoir $m_D(r_{eD}, t_D) = 0$,

3) exponential $r_D \frac{\partial m_D}{\partial r_D}|_{r_D=\infty} = -q_{ext}(1-e^{\frac{t_D}{\tau_D}})$ and

4) power law $r_D \frac{\partial m_D}{\partial r_D}|_{r_D=\infty} = -q_{ext} H(t_D - 1)(1-t_D{}^{-\alpha})$.

For the first boundary condition (BC1), when $r \to \infty$ then $k_0 \to 0$, $I_0 \to \infty$, hence to satisfy $\overline{m}_D(r_D \to \infty, t_D) = 0$, c_1 should be equal to zero for delamination of I_0 effect, then for this boundary condition, the Eq. (23) reduces to,

$$\overline{m}_D = c_2 k_0(w) \tag{24}$$

For the second boundary condition (BC2), $m_D(r_{eD}, t_D) = 0$ then $\overline{m}_D(r_{eD}, t_D) = 0$, by substituting this boundary condition the equation (23) becomes,

$$\overline{m}_D = c_1 I_0(w_{r_{eD}}) + c_2 k_0(w_{r_{eD}}) = 0 \tag{25}$$

For the third outer boundary condition (BC3), $r_D \frac{\partial m_D}{\partial r_D}|_{r_D=\infty} = -q_{ext}(1 - e^{-\frac{t_D}{\tau_D}})$ then $w \frac{\partial \overline{m}_D}{\partial w}|_{r_{eD}} = -q_{ext}(\frac{1}{s} - \frac{\tau_D}{\tau_D s + 1})$, by substituting this boundary condition the equation (23) becomes,

$$w \frac{\partial \overline{m}_D}{\partial w}|_{r_{eD}} = c_1 \sqrt{\frac{s}{B}} r_{eD} I_1(w_{r_{eD}}) - \tag{26}$$
$$c_2 \sqrt{\frac{s}{B}} r_{eD} k_1(w_{r_{eD}}) = -q_{ext}(\frac{1}{s} - \frac{\tau_D}{\tau_D s + 1})$$

For outer boundary condition of 4 (BC4), $r_D \frac{\partial m_D}{\partial r_D}|_{r_D=\infty} = -q_{ext} H(t_D - 1)(1-t_D{}^{\alpha})$ then for $t_D > 1$, $w \frac{\partial \overline{m}_D}{\partial w}|_{r_D=\infty} = -q_{ext}(\frac{1}{s} - \frac{\Gamma(\alpha+1)}{s^{\alpha+1}})$, by substituting this boundary condition the equation (23) becomes

$$w \frac{\partial \overline{m}_D}{\partial w}|_{r_{eD}} = c_1 \sqrt{\frac{s}{B}} r_{eD} I_1(w_{r_{eD}}) - \tag{27}$$
$$c_2 \sqrt{\frac{s}{B}} r_{eD} k_1(w_{r_{eD}}) = -q_{ext}(\frac{1}{s} - \frac{\Gamma(-\alpha+1)}{s^{-\alpha+1}})$$

Four Equation of (24) to (27), all outer boundary condition been applied. Now the inner boundary condition should be applied. The inner boundary condition is $r_D \frac{\partial \Delta m_D}{\partial r_D}|_{r_D=1} = -1$, hence $w \frac{\partial \overline{m}_D}{\partial w}|_{r_D=1} = -\frac{1}{s}$, by substituting this boundary condition the Eq. (23) becomes

$$w \frac{\partial \overline{m}_D}{\partial w}\Big|_{w_{r_D=1}} = c_1 \sqrt{\frac{s}{B}} I_1(w_{r_D=1}) - \tag{28}$$
$$c_2 \sqrt{\frac{s}{B}} k_1(w_{r_D=1}) = -\frac{1}{s}$$

Then, by solving for any outer boundary condition along with the inner boundary condition, both c_1 and c_2 are determined. The c_1 and c_2 parameter for different boundary condition in Equation (23) through solving pair of Equations of (28) and (24), (28) and (25), (28) and (26), (28), and (27) are listed in Table 1.

Stehfest numerical Laplace inversion is used to calculate Eq. (23).

$$m_w(r_D, t_D) = \frac{\ln 2}{t_D} \sum_{i=1}^{N} V_i \overline{m}_w(r_D, s_i) \tag{29}$$

Where the V_i can be calculated as follow,

$$V_i = (-1)^{\left\{\frac{N}{2}+i\right\}} \sum_{k=\left[\frac{1+1}{2}\right]}^{\min\left\{\frac{N}{2}, i\right\}} \frac{k^{\frac{N}{2}+1} * (2k)!}{\left[\frac{N}{2} - k\right]! * (k!)^2 (i-k)! (2k-i)!} \tag{30}$$

The wellbore storage (C_D) and skin factor (S_k) effect in the Laplace space can be considered as follow [17],

$$\overline{m}_{WDs} = \frac{\overline{m}_D + \frac{S_k}{s}}{1 + C_D s(\overline{m}_D + \frac{S_k}{s})} \tag{31}$$

Table 1: c_1 and c_2 parameter for different boundary condition in Eq. (23).

Boundary condition	c_1	c_2
1	0	$c_2 = \frac{1}{s\sqrt{s/B}k_1(\sqrt{s/B})}$
2	$\frac{-k_0(\sqrt{s/B}r_{eD})}{s\sqrt{s/B}*(I_0(\sqrt{s/B}r_{eD})k_1(\sqrt{s/B})+I_1(\sqrt{s/B})k_0(\sqrt{s/B}r_{eD})}$	$\frac{I_0(\sqrt{s/B}r_{eD})}{s\sqrt{s/B}*(I_0(\sqrt{s/B}r_{eD})k_1(\sqrt{s/B})+I_1(\sqrt{s/B})k_0(\sqrt{s/B}r_{eD})}$
3	$\frac{-r_{eD}k_1(\sqrt{s/B}r_{eD})(1+s\tau_D)+q_{ext}k_1(\sqrt{s/B})}{s\sqrt{s/B}r_{eD}(1+s\tau_D)\left[I_1(\sqrt{s/B})k_1(\sqrt{s/B}r_{eD})-I_1(\sqrt{s/B}r_{eD})k_1(\sqrt{s/B})\right]}$	$\frac{-r_{eD}I_1(\sqrt{s/B}r_{eD})(1+s\tau_D)+q_{ext}I_1(\sqrt{s/B})}{sr_{eD}\sqrt{s/B}(1+s\tau_D)\left[I_1(\sqrt{s/B})k_1(\sqrt{s/B}r_{eD})-I_1(\sqrt{s/B}r_{eD})k_1(\sqrt{s/B})\right]}$
4	$\frac{q_{ext}(1-\Gamma(-\alpha+1)*s^{\alpha})k_1(\sqrt{s/B})-k_1(\sqrt{s/B}r_{eD})r_{eD}}{r_{eD}s\sqrt{s/B}\left[I_1(\sqrt{s/B})k_1(\sqrt{s/B}r_{eD})-I_1(\sqrt{s/B}r_{eD})k_1(\sqrt{s/B})\right]}$	$\frac{q_{ext}(1-\Gamma(-\alpha+1)*s^{\alpha})I_1(\sqrt{s/B})-I_1(\sqrt{s/B}r_{eD})r_{eD}}{r_{eD}s\sqrt{s/B}\left[I_1(\sqrt{s/B})k_1(\sqrt{s/B}r_{eD})-I_1(\sqrt{s/B}r_{eD})k_1(\sqrt{s/B})\right]}$

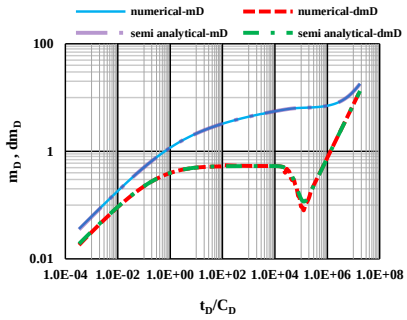

Fig. 1: Comparision of the numerical and semi-analytical solution. For C_D=0, S_k=0, q_{ext}=0.9, τ_D=10000, and reD=1000.

RESULTS AND DISCUSSIONS

To validate the semi-analytical solution, numerical solution through fully implicit finite difference discretizing of the partial differential equation of (19) has been obtained. All the equations were coded and solved in MATLAB 2017-b software. Comparison of pressure response and its derivative of the numerical and semi-analytical solutions showed a good agreement between the two approaches. For summarizing, the mentioned comparison only for time-dependent flow boundary condition (BC3), exponential boundary condition, is depicted in Fig. 1. Based on this comparison, one can conclude that the developed semi-analytical method is valid for the creation of type curves and consequently some interpretation.

The effect of different outer Boundary Conditions (BC1, BC2, BC3, and BC4) on the pressure response of the reservoir is showed in Fig. 2. In BC1, an infinite-acting reservoir with a constant pressure derivative of 0.5 is obvious. In BC2, the outer boundary has a constant pressure; then it is expected that the pressure response when it arrives at the outer boundary would cause the derivative of pressure inclines to zero. In the BC3 and BC4 after an initial decrease, the pressure derivative will tend to increase.

The pressure reaction of a reservoir for a single well with a constant production surface flow rate and variable flow at the external boundary (BC3) for different values of τ_D is shown in Fig. 3. This figure shows the result of the semi-analytical solution of equation (23) by applying BC3 for τ_D=0 and τ_D=10^8. It is obvious that increasing the effect of flow (lower τ_D) causes an initial decrease in pressure derivative, then a constant increase. When τ_D tends to zero, the boundary condition becomes $\frac{\partial m_D}{\partial r_D}|_{r_D=\infty} = cte$. For high τ_D, reservoir act like a fractured reservoir which its characteristic is two straight parallel lines in dimensionless pressure versus dimensionless time [36-38]. When τ_D tends to infinite, the boundary condition becomes $\frac{\partial m_D}{\partial r_D}|_{r_D=\infty} = 0$.

The influence of α on the type curve of BC4 is shown in Fig. 4. It could be concluded that the pseudo-steady state flow regime is influenced by α value. It is noteworthy that as α tends to zero the effect of external boundary condition

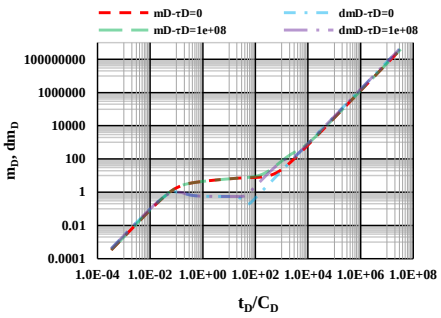

Fig. 2: Effect of different outer boundary condition on the dimensionless pseudo pressure and its derivative curve. For all boundary conditions: C_D=3, S_k=1, for BC1, BC2, BC3: r_{eD}= 1000, for BC2 and BC3: q_{ext}= 0.5, for BC3: τ_D = 10000, for BC4: α = 0.5.

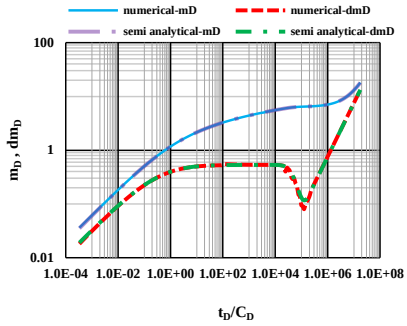

Fig. 3: Effect of τ_D on the dimensionless pseudo pressure and its derivative type curve of the non-condensate gas reservoir with exponential flux boundary conditions. : C_D=3, S_k=1, r_{eD}= 1000, q_{ext}= 0.8.

on the dimensionless pseudo pressure curve and its derivative becomes unimportant. In this condition, the reservoir acts like a finite reservoir with a closed boundary condition which can be detected by a united slope in pressure response and its derivative. When a reservoir is closed in all directions, the pressure response moves toward the reservoir boundary until it reaches the boundary. Then, the reservoir pressure decline enters the pseudo-steady state condition. In this situation, the reservoir pressure at any point decreases at a constant rate [39].

Fig. 5 shows the effect of gas slippage on the type curve of the reservoir with exponential flux boundary conditions. It is obvious that it has no effect on the general form of type curve and it just causes a faster arrival of pressure response to the boundary. Then it can be concluded that in a Non-Condensate gas reservoir with Knudsen number larger than 0.1, slippage will cause a sooner observation of boundary effect.

A time-dependent flux at the external boundary for BC1 or BC2 in the Non-Condensate gas reservoir shows that the period of flow regime dominated by the external boundary flow is different considerably from a Non-Condensate gas reservoir with zero flux at the external boundary.

Finally, the flow regimes can be categorized into the following steps,

Step 1: The early effects of wellbore storage, also known as after flow or after production, which is distinguished by unit slop line in a log-log plot of both the pseudo-pressure and derivative pseudo-pressure versus dimensionless time. In the condition that wellbore storage is significant, it must be considered to avoid misinterpretation of results.

Step 2: The transition behavior from wellbore storage to the radial regimes of the reservoir. The pseudo-pressure derivative curves versus dimensionless time in a log-log plot in this period are similar to hump. The S_k and hump height has a direct relationship. There are different ways to determine wellbore improvement or damage. For this purpose, the pressure response can be used. An improved well shows a trough, a negative skin factor, while damaged wells show hump, a positive skin factor.

Step 3: Radial flow period of the reservoir, which is distinguished by a horizontal straight line with the value of 0.5 for the dimensionless pseudo pressure derivative curve versus dimensionless time in a log-log plot. This flow period can only be distinguished when the radial flow regime is much larger than the effect of skin factor and wellbore storage.

Step 4: The transition flow between external boundary conditions and radial flow periods of the reservoir. The boundary effect (q_{ext}, α, τ_D, $m_D(r_{eD},0)$) will control the behavior of this region. For BC1, because of the infinity of the reservoir, this step is not to be seen. For BC2, a constant decrease in on dimensionless pseudo pressure derivative curve versus dimensionless time in a log-log

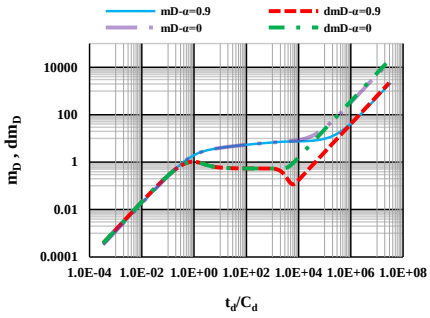

Fig. 4: Effect of α on the dimensionless pseudo pressure and its derivative type curve of the non-condensate gas reservoir with power-law flux boundary conditions. C_D=3, S_k=1, r_{eD}= 1000, and q_{ext}= 0.5.

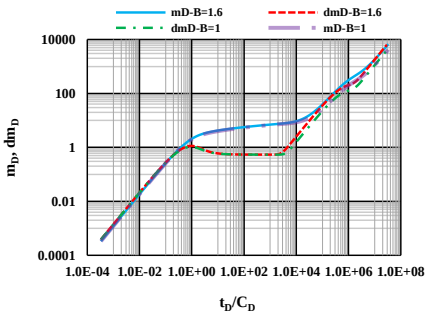

Fig. 5: Effect of gas slippage on the dimensionless pseudo pressure and its derivative type curve on the non-condensate gas reservoir with exponential flux boundary conditions. C_D=3, S_k=1, r_{eD}= 1000, τ_D = 1e+0.8 and q_{ext}= 0.8.

the plot is observable. This transient region for BC3 is dependent on the combination of parameters. There may be a trough on dimensionless pseudo pressure derivative curve versus dimensionless time or two parallel lines like a naturally fractured reservoir on both dimensionless pseudo pressure and dimensionless pseudo pressure derivative curve versus dimensionless time in a log-log plot. For BC4 a trough for low values of α on dimensionless pseudo pressure derivative curve versus dimensionless time in a log-log plot can be seen.

Step 5: the steady-state flow period for BC2 and the pseudo-steady state flow period in BC3 and BC4.

CONCLUSIONS

In this study, a semi-analytical solution for a Non-Condensate gas reservoir with a single well producing at a constant flow rate with four different boundary conditions along with gas slippage effect, wellbore storage effect, and skin factor has been derived. External boundary conditions considered as an infinite reservoir, constant pressure, exponential variable flux, and power-law variable flux. For the solution of finial derived equation, the numerical Laplace transform has been utilized and the results been compared with the finite difference numerical solution of the partial differential equation of modeled reservoir to verify the semi-analytical solution. Models exhibit in general, six flow regimes: wellbore storage effect, skin effect, first transition flow period, radial flow period, second transition flow period, and boundary controlled flow period. The studied models may help to a better understanding and appreciating the conventional well:

Testing analysis for a single well Non-Condensate gas reservoir with external boundary conditions.

Nomenclature

ρ	Density, kg/m^3
Φ	Porosity
V	The volume of the element, m^3
t	Time, s
q	Flow, m^3/s
A_r	The cross-section area, m^2
k_a	Apparent permeability
k_∞	Absolute permeability
μ	Viscosity
B	The coefficient of dependent to Knudsen
f	A function dependent on the Knudsen number
K_n	Knudsen number
M	Gas molecular weight
R	Universal constant of the gas
T	Temperature
z_g	Deviation factor of gas
m	Gas pseudo pressure
V_i	Variable of Laplace inversion
C_D	Wellbore storage
S_k	Skin factor
t_D	Dimensionless time
m_D	Dimensionless pseudo pressure
r_D	Dimensionless radius

r	Radius, m
m	Pseudo pressure (defined in Equation (11))
P	Pressure, N/m^2
K	Permeability, m^2
h	Thickness
dr	Element width

Received : May. 7, 2019 ; Accepted : Sep. 16, 2019

REFERENCES

[1] Pascal H., Pascal F., Flow of Non-Newtonian Fluid Through Porous Media, *International Journal of Engineering Science*, **23(5)**: 571-585 (1985).

[2] Dabiri Atashbeyk M., Shahbazi K., Fattahi M., Pressure Profile Estimation through CFD in UBD Operation Considering with Influx to Wellbore, *Iranian Journal of Chemistry and Chemical Engineering (IJCCE)*, **37(6)**: 271-283 (2018).

[3] Barzegar F., Azadi Tabar M., Masihi M., New Method of Generating and Clustering Pore Network Model, *Oil Geomechanic*, **3(2)**: 1-17 (2019).

[4] Ahmed T., "Reservoir Engineering Handbook", 3rd ed., Houton, Texas, (2006).

[5] Azadi Tabar M., Barzegar F., Ghazanfari M.H., Mohammadi M., On the Applicability Range of Cassie–Baxter and Wenzel Equation: a Numerical Study, *Journal of the Brazilian Society of Mechanical Sciences and Engineering*, **41(10)**: 399- 399 (2019).

[6] Aziz K., Settari A., "Petroleum Reservoir Simulation", Chapman & Hall, (1979).

[7] Azadi Tabar M., Ghazanfari M.H., Experimental Study of Surfapore Nanofluid Effect on Surface Free Energy of Calcite Rock, (in eng), *Modares Mechanical Engineering*, **19(3)**: 709-718 (2019).

[8] Azadi Tabar M., Ghazanfari M.H., Monfared A.D., On the Size-Dependent Behavior of Drop Contact Angle in Wettability Alteration of Reservoir Rocks to Preferentially Gas Wetting Using Nanofluid, *Journal of Petroleum Science and Engineering*, **178**: 1143-1154 (2019).

[9] Zhao Y.-l., Zhang L.-h., Zhao J.-z., Luo J.-x., Zhang B.-n., Triple porosity Modeling of Transient Well Test and Rate Decline Analysis for Multi-Fractured Horizontal Well in Shale Gas Reservoirs, *Journal of Petroleum Science and Engineering*, **110**: 253-262 (2013).

[10] Bahrami H., Siavoshi J., Interpretation of Reservoir Flow Regimes and Analysis of Welltest Data in Hydraulically Fractured Unconventional Oil and Gas Reservoirs, in: *SPE Unconventional Gas Conference and Exhibition"*, Society of Petroleum Engineers (2013).

[11] Spivey J.P., Lee W.J., "Applied Well Test Interpretation", Society of Petroleum Engineers Richardson, TX, (2013).

[12] Xu S., Lee W.J., Two-Phase Well Test Analysis of Gas Condensate Reservoirs, in: "*SPE Annual Technical Conference and Exhibition"*, Society of Petroleum Engineers (1999).

[13] Earlougher R.C., "Advances in Well Test Analysis", Henry L. Doherty Memorial Fund of AIME New York, (1977).

[14] Gringarten A.C., Ramey Jr H.J., Raghavan R., Unsteady-State Pressure Distributions Created by a Well with a Single Infinite-Conductivity Vertical Fracture, *Society of Petroleum Engineers Journal*, **14(04)**: 347-360 (1974).

[15] Ertekin T., Abou-Kassen J.H., King G.R., "Basic Applied Reservoir Simulations", Society of Petroleum Engineers, (2001).

[16] von Rosenberg D.U., Local Mesh Refinement for Finite Difference Methods, in: "*SPE Annual Technical Conference and Exhibition"*, Society of Petroleum Engineers (1982).

[17] Zhao Y.-L., Zhang L.-H., Liu Y.-h., Hu S.-Y., Liu Q.-G., Transient Pressure Analysis of Fractured Well in Bi-Zonal Gas Reservoirs, *Journal of Hydrology*, **524**: 89-99 (2015).

[18] Azadi Tabar M., Mohammadi M., Jamshidi S., Hydraulically Fractured Bi-zonal Gas Reservoir Well Testing Using Dimensionless Numerical Simulation, *Journal of Petroleum Research*, **27(96-6)**: 32-45 (2018).

[19] Acosta L., Ambastha A., Thermal Well Test Analysis Using an Analytical Multi-Region Composite Reservoir Model, in: "*SPE Annual Technical Conference and Exhibition*": Society of Petroleum Engineers (1994).

[20] Earlougher Jr R.C., Kersch K., Kunzman W., Some Characteristics of Pressure Buildup Behavior in Bounded Multiple-Layered Reservoirs without Crossflow, *Journal of Petroleum Technology*, **26(10)**: 1178-1186 (1974).

[21] Corbett P.W., Hamdi H., Gurav H., Layered Fluvial Reservoirs with Internal Fluid Cross Flow: A Well-Connected Family of Well Test Pressure Transient Responses, *Petroleum Geoscience*, **18(2)**: 219-229 (2012).

[22] Doublet L., Blasingame T., "Decline Curve Analysis Using Type Curves: Water Influx/Waterllood Cases," *SPE Paper*, pp. 22-25 (1995).

[23] Veyskarami M., Hassani A.H., Ghazanfari M.H., "A New Insight Into Onset of Inertial Flow in Porous Media Using Network Modeling with Converging/Diverging Pores," Computational Geosciences, pp. 1-18, (2017).

[24] Freeman C., Moridis G., Blasingame T., A Numerical Study of Microscale Flow Behavior in Tight Gas and Shale Gas Reservoir Systems, *Transport in Porous Media*, **90(1)**: 253 (2011).

[25] Holditch S.A., Tight Gas Sands, *Journal of Petroleum Technology*, **58(06)**: 86-93 (2006).

[26] Nelson P.H., Pore-Throat Sizes in Sandstones, Tight Sandstones, and Shales, *AAPG Bulletin*, **93(3)**: 329-340 (2009).

[27] Falk K., Coasne B., Pellenq R., Ulm F.-J., Bocquet L., Subcontinuum Mass Transport of Condensed Hydrocarbons in Nanoporous Media, *Nature Communications*, **6**: 1-7 (2015).

[28] Clarkson C.R., Solano N., Bustin R. M., Bustin A.M.M., Chalmers G.R.L., He L., Melnichenko Y.B., Radliński A.P., Blach T.P., Pore Structure Characterization of North American Shale Gas Reservoirs Using USANS/SANS, Gas Adsorption, and Mercury Intrusion, *Fuel*, **103**: 606-616 (2013).

[29] Wang L., Zhang Ronglei, Wang Cong, Xiong Yi, Zheng Xishen, Li Shangru, Jin Kai, Rui Zhenhua, Review of Multi-Scale and Multi-Physical Simulation Technologies for Shale and Tight Gas Reservoirs, *Journal of Natural Gas Science and Engineering*, **37**: 560-578 (2017).

[30] Javadpour F., Fisher D., Unsworth M., Nanoscale Gas Flow in Shale Gas Sediments, *Journal of Canadian Petroleum Technology*, **46(10)**: 55-61 (2007).

[31] Ziarani A.S., Aguilera R., Knudsen's Permeability Correction for Tight Porous Media, *Transport in Porous Media*, **91(1)**: 239-260 (2012).

[32] Civan F., Effective Correlation of Apparent Gas Permeability in Tight Porous Media, *Transport in Porous Media*, **82(2)**: 375-384 (2010).

[33] Veyskarami M., Hassani A.H., Ghazanfari M.H., Modeling of Non-Darcy Flow Through Anisotropic Porous Media: Role of Pore Space Profiles, *Chemical Engineering Science*,**151**: 93-104 (2016).

[34] Gerald C.F., Wheatley P.O., "Applied Mumerical Analysis", Addison-Wesley Reading, MA, (1984).

[35] Abramowitz M., Stegun I.A., "Handbook of Mathematical Functions: with Formulas", Graphs, and Mathematical Tables, Courier Corporation (1964).

[36] H. Cinco-Ley, Well-Test Analysis for Naturally Fractured Reservoirs, *Journal of Petroleum Technology*, **48(01)**: 51-54 (1996).

[37] Saidi A.M., "Reservoir Engineering of Fractured Reservoirs (fundamental and Practical Aspects)", Total (1987).

[38] Da Prat G., "Well Test Analysis for Fractured Reservoir Evaluation", Elsevier, (1990).

[39] Lee J., "Well Testing, Society of Petroleum Engineers", (1982).

Ref 39 is a book, hence there is no more information for it.s :[\] Commented [MAT